

# Stochastic resonance induced by an unknown linear frequency modulated signal in a strong noise background

Cite as: Chaos **30**, 043128 (2020); <https://doi.org/10.1063/5.0002134>

Submitted: 22 January 2020 . Accepted: 07 April 2020 . Published Online: 20 April 2020

Chengjin Wu, Jianhua Yang , Miguel A. F. Sanjuán , and Houguang Liu



View Online



Export Citation



CrossMark

## ARTICLES YOU MAY BE INTERESTED IN

[Maximum entropy principle in recurrence plot analysis on stochastic and chaotic systems](#)

Chaos: An Interdisciplinary Journal of Nonlinear Science **30**, 043123 (2020); <https://doi.org/10.1063/1.5125921>

[Using nanoresonators with robust chaos as hardware random number generators](#)

Chaos: An Interdisciplinary Journal of Nonlinear Science **30**, 043126 (2020); <https://doi.org/10.1063/5.0004703>

[Ultraviolet solar flare signatures in the framework of complex network](#)

Chaos: An Interdisciplinary Journal of Nonlinear Science **30**, 043124 (2020); <https://doi.org/10.1063/1.5129433>



YOUR WORK ILLUMINATES NEW POSSIBILITIES  
LET US HELP IT SHINE

Learn more 



# Stochastic resonance induced by an unknown linear frequency modulated signal in a strong noise background

Cite as: Chaos 30, 043128 (2020); doi: 10.1063/5.0002134

Submitted: 22 January 2020 · Accepted: 7 April 2020 ·

Published Online: 20 April 2020



View Online



Export Citation



CrossMark

Chengjin Wu,<sup>1,2</sup> Jianhua Yang,<sup>1,2,a)</sup> Miguel A. F. Sanjuán,<sup>3,4</sup> and Houguaug Liu<sup>1</sup>

## AFFILIATIONS

<sup>1</sup>School of Mechatronic Engineering, China University of Mining and Technology, Xuzhou 221116, People's Republic of China

<sup>2</sup>Jiangsu Key Laboratory of Mine Mechanical and Electrical Equipment, China University of Mining and Technology, Xuzhou 221116, People's Republic of China

<sup>3</sup>Nonlinear Dynamics, Chaos and Complex Systems Group, Departamento de Física, Universidad Rey Juan Carlos, Tulipán s/n, 28933 Móstoles, Madrid, Spain

<sup>4</sup>Department of Applied Informatics, Kaunas University of Technology, Studentu 50-407, Kaunas 51368, Lithuania

<sup>a)</sup>Author to whom correspondence should be addressed: [jianhuayang@cumt.edu.cn](mailto:jianhuayang@cumt.edu.cn)

## ABSTRACT

Stochastic resonance (SR) is widely used as a signal enhancement technique in recovering and enhancing periodic or aperiodic signals submerged in noise. However, system parameters and noise intensity tend to influence the SR performance. To achieve better resonance performance, several indices are often used to determine these parameters, including signal-to-noise, amplification factor, and cross-correlation coefficient. Nevertheless, for a linear frequency modulated (LFM) signal, such indices may no longer work and consequently make SR unable to recover the unknown LFM signal from raw signals. Thus, this limits the application of SR to some extent. To deal with this problem, we define here a new index to characterize the unknown LFM signal with the help of the fractional Fourier transform. Guided by this index, SR is thus able to recover the unknown LFM signal from the raw signal. In addition, a cloud model based genetic algorithm is used to achieve an adaptive SR in order to improve the effectiveness of signal processing.

Published under license by AIP Publishing. <https://doi.org/10.1063/5.0002134>

Stochastic resonance (SR) is a dynamic phenomenon that exploits the positive effect of the noise to enhance a weak signal and reduces noise, which attracts much attention. Compared with traditional denoising techniques, SR will not weaken the internal signal. Owing to this distinguishing feature, SR has been constantly developed and it can not only process periodic signals but also aperiodic signals. Although SR is able to process many kinds of signals, it is difficult for SR to recover the unknown linear frequency modulated (LFM) signal, which is completely hidden in the noise background. On the one hand, the instantaneous frequency of the LFM signal linearly varies with time so that the system of SR cannot match the signal well. On the other hand, the LFM signal submerged in noise is hardly characterized and identified, but the LFM signal commonly occurs in the signal processing field. Hence, it is urgent to achieve its recovery from noise by SR. In addition, parameter selection is another factor that limits the application of SR so that an adaptive SR theory needs to be

further developed through an excellent optimization algorithm. As a result, this study intends to handle these problems in order to achieve quickly the recovery of the unknown LFM signal.

## I. INTRODUCTION

Stochastic resonance (SR) is a phenomenon in a nonlinear system where an appropriate dose of noise can enhance a weak signal in the response. It was first proposed by Benzi *et al.*<sup>1</sup> to explain the periodic recurrence of ice ages. Once it was proposed and observed, it has attracted much attention. Afterward, many important results on SR have been found in the past three decades so that a SR theory has been developed gradually and perfected. To date, due to its excellent performance, SR has been applied into many areas, including biology,<sup>2-4</sup> chemistry,<sup>5,6</sup> physics,<sup>7</sup> and so forth. In recent years, scholars mainly focus on the application of SR in signal processing,

and many results have been found.<sup>8–10</sup> Initially, SR was only used to process a low-frequency harmonic signal where the orders of magnitude of the system parameters are 1. In this case, the SR is usually named small parameters SR. Then, to develop the application of SR from low-frequency to high-frequency, researchers proposed some techniques, such as normalized scale transformation and general scale transformation.<sup>11</sup> Based on these techniques, SR can manage to process high-frequency signals, and thus SR can be applied in engineering fields, e.g., fault diagnosis of rotary machines.<sup>12–15</sup>

SR not only can process the signals with a harmonic component but also aperiodic signals, such as aperiodic binary signals. SR has been used to implement base-band binary signal transmission,<sup>16–18</sup> image processing,<sup>19</sup> and optical cavities.<sup>20</sup> However, besides the aperiodic binary signals, there are some other kinds of aperiodic signals that need to be processed, especially frequency modulated signals. This is because modulation phenomena commonly occur in the scientific and engineering fields. One of the most important signals in frequency modulated signals is the linear frequency modulated (LFM) signal.<sup>21–24</sup> In fact, some characteristic signals have the same characteristic as the LFM signal, for example, the vibration fault signal of a faulty bearing when rotation speed is linearly rising. Owing to its importance, many research studies have been conducted and meanwhile some important results have been obtained.<sup>25–28</sup>

Although some important results have been reported, there are still many problems worthy of further research. Different from the harmonic signal, the instantaneous frequency of the LFM signal turns large as time goes. So, the frequency spectrum of the LFM signal has a certain bandwidth. On the one hand, this will lead to the issue that SR is hard to apply because the system of SR cannot match well the LFM signal. On the other hand, when the LFM signal is submerged in a strong noise background, it is difficult to use several common indices, including signal-to-noise, cross-correlation coefficient, and amplification factor, to characterize the LFM signal. This is because the information on the waveform and frequency of the hidden LFM signal is usually unknown in this case. Therefore, nowadays, there is no appropriate index to help characterize the LFM signal in the noise. Motivated by these issues, this work aims at proposing a new index in order to recover the hidden LFM signal from the raw signal.

As is well known, system parameters and noise intensity are the factors affecting the SR performance. So, parameter selection has been a problem leading to SR hard to be widely applied. Fortunately, many algorithms have been proposed that can solve a lot of optimization problems. Among them, cloud model based genetic algorithm (CMGA) is a kind of optimization algorithm that has a good global search ability and a fast convergence speed.<sup>29–31</sup> As a result, CMGA is used for the parameter optimization of SR with an excellent performance of the algorithm, in order to achieve an adaptive SR.

The rest of this paper is organized as follows. In Sec. II, the re-scaled SR theory and the proposed index are introduced and explained in detail. In addition, several related numerical simulations are carried out in order to verify the effectiveness of the index. In Sec. III, the adaptive SR based on CMGA is achieved to improve the SR performance on processing the LFM signal. Finally, the main conclusions are provided in Sec. IV.

## II. THEORETICAL FORMULATION AND NUMERICAL SIMULATION

In this part, we first introduce the classic SR and the re-scaled SR theory, and then we give a specific expression of the proposed index. At last, some simulations demonstrate the process of recovering an unknown LFM signal based on the index.

### A. The re-scaled SR theory and the proposed index

Considering a typical bistable system, the classic SR can be described by

$$\frac{dx}{dt} = ax - bx^3 + s(t) + N(t), \quad (1)$$

in which  $a$  and  $b$  are the system parameters ( $a > 0$ ,  $b > 0$ ). The function  $s(t)$  is the LFM signal,

$$s(t) = A\cos(\pi\gamma t^2 + 2\pi f_0 t + \phi), \quad (2)$$

where  $A$  is its amplitude,  $\gamma$  is its chirp rate,  $f_0$  is its centroid frequency, and  $\phi$  is its initial phase. The function  $N(t)$  is a Gaussian white noise with the following statistical properties:

$$\langle N(t) \rangle = 0, \quad \langle N(t), N(0) \rangle = 2D\delta(t), \quad (3)$$

where  $D$  denotes the noise intensity of the additive noise.

As is well known, the instantaneous frequency of the LFM signal rises with the increase in time. This means that the frequency variation may make the classic SR hard to induce the LFM signal. Thus, it is necessary to introduce the general scale transformation method into SR. For this purpose, we make

$$\tau = \beta t, \quad z(\tau) = x(t), \quad (4)$$

where  $\beta$  is the time scale. Substituting Eq. (4) into Eq. (1), we can obtain

$$\frac{dz(\tau)}{d\tau} = \frac{a}{\beta}z(\tau) - \frac{b}{\beta}z^3(\tau) + \frac{1}{\beta}s\left(\frac{\tau}{\beta}\right) + \frac{1}{\beta}N\left(\frac{\tau}{\beta}\right). \quad (5)$$

Now, by multiplying the right-hand side of Eq. (5) by  $\beta$ , the equation becomes

$$\frac{dz(\tau)}{d\tau} = az(\tau) - bz^3(\tau) + s\left(\frac{\tau}{\beta}\right) + N\left(\frac{\tau}{\beta}\right). \quad (6)$$

From Eq. (6), we can see that it meets the precondition of small parameter SR. In other words, according to the equation, SR is able to occur. Letting

$$t = \frac{\tau}{\beta}, \quad x(t) = z(\tau), \quad (7)$$

then we obtain

$$\frac{dx(t)}{dt} = \beta ax - \beta bx^3 + \beta s(t) + \beta N(t). \quad (8)$$

As is well known, scale transformation will not change the dynamic properties of the system. Therefore, this means that by using Eq. (8), we can induce SR with a high-frequency signal.

Fractional Fourier transform (FRFT) is a common method used to process the LFM signal. FRFT of  $x(t)$  is defined as

$$X_p(u) = F^p[x(t)] = \int_{-\infty}^{\infty} x(t)K_\alpha(t, u)dt, \quad (9)$$

where  $p$  is the order of FRFT,  $F^p[\cdot]$  is the operator, and  $K_\alpha(t, u)$  is the kernel of the FRFT described as

$$K_\alpha(t, u) = \begin{cases} \sqrt{\frac{1-j\cot\alpha}{2\pi}} (\exp j\frac{t^2+u^2}{2} \cot\alpha - tu\alpha), & \alpha \neq n\pi, \\ \delta(t-u), & \alpha = 2n\pi, \\ \delta(t+u), & \alpha = (2n \pm 1)\pi, \end{cases} \quad (10)$$

in which  $j$  is the imaginary unit ( $j^2 = -1$ ) and  $\alpha$  is the rotation angle of axis ( $\alpha = p\pi/2$ ). As a result, through FRFT, the signal  $x(t)$  can be transformed into  $X(u)$  in the fractional Fourier domain. During this process, if  $\alpha$  is selected properly, then the LFM signal can be transformed into an impulse. This means that FRFT brings about the concentration of the energy of the LFM signal. However, the noise energy cannot be focused in the fractional Fourier domain.

SNR is a kind of index that describes the relationship between the signal energy at a specific frequency and the noise energy. In many studies on SR, SNR is the most common index used to characterize the signal energy at a fixed frequency. However, since the instantaneous frequency of the LFM signal keeps changing with time, there is a frequency band with a certain bandwidth, which describes the signal energy in the frequency domain. Due to the effect of noise, it is difficult to continue to use the SNR to accurately describe the relationship between the signal energy at a frequency band and the noise energy. Therefore, in this paper, we define a new index, which we call *fractional signal-to-noise ratio* (FSNR), that we define as

$$FSNR = 10 \log \frac{|X(u_p)|^2}{\sum_{u=1}^N |X(u)|^2 - |X(u_p)|^2}. \quad (11)$$

Herein,  $|X(u_p)|^2$  is the LFM signal energy and  $(\sum_{u=1}^N |X(u)|^2) - |X(u_p)|^2$  is the noise energy in optimal fractional domain.

### B. Numerical simulations

Here, we present several groups of raw signals as shown in Fig. 1. From top to bottom, the amplitudes of the LFM signals are 0.1, 0.2, and 0.3, and they have been submerged by noise with a 0.2 noise intensity. To verify the effectiveness of FSNR in SR, it will be used to process these signals.

At first, to calculate FSNR, raw signals need to be processed through FRFT. The results after processing are shown in Fig. 2. In the first subplot, the amplitude spectra for different orders are plotted. It can be seen that there is a distinct peak appearing in the  $(p, u)$  plane. Corresponding to the peak, the amplitude spectrum at optimal order is depicted in the second subplot. Apparently, the LFM signal contained in the raw signal is turned into an impulse in  $u$  domain but the noise is not. Therefore, according to the definition of the index, the value of FSNR for the signal can be easily calculated, which is 18.05.

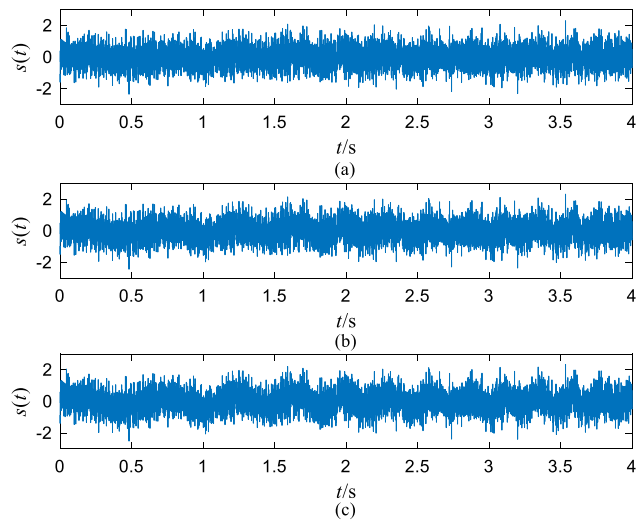


FIG. 1. Several groups of noisy raw signals with a 0.2 noise intensity. The simulation parameters are  $\gamma = 1$ ,  $f_0 = 1$ , and  $\varphi = 0$ . (a)  $A = 0.1$ , (b)  $A = 0.2$ , and (c)  $A = 0.3$ .

Then, based on this index, it can be used to measure the SR output so that several parameters are able to be determined, such as the noise intensity or the system parameters. In the SR theory, adding some noise is able to make the system to have a better output. Thus, by letting the noise intensity to be an independent variable, we can compute the FSNR vs the noise intensity for three different raw signals, as shown in Fig. 3. Initially, the value of the FSNR is comparatively low when there is no noise added into the system. At this moment, the SR is not enough to be induced only by the noise within the raw signal. Next, as the noise intensity increases, each curve rises and then peaks at a certain point. Finally, the curve falls slowly when more and more noise is input into the system. The point is often called resonance point where SR tends to occur.

Figure 4 illustrates the phenomena at resonance points, showing the system outputs and the fitted signals. Compared with the signals in Fig. 1, the LFM signal hidden by noise can be recognized. In addition, the hidden LFM signal has been enhanced, which means the noise energy almost has been transferred into the LFM signal and obviously SR is able to happen. It indicates that the SR almost occurs when the FSNR reaches a local maximum.

Furthermore, taking the FRFT of the system outputs and rotating the outputs at an optimal angle, Fig. 5 is obtained. It can be seen that there are only signal frequency components left in the fractional Fourier domain, but the noise is almost removed. This also indicates that the FSNR affords to measure and characterize the SR output.

### III. THE ADAPTIVE SR BASED ON OPTIMIZATION ALGORITHM

In this section, we first briefly introduce the specific theory and the implementation process on CMGA. Then, with the help of the algorithm, an adaptive SR can be achieved in order to obtain the recovery of the LFM signal quickly.

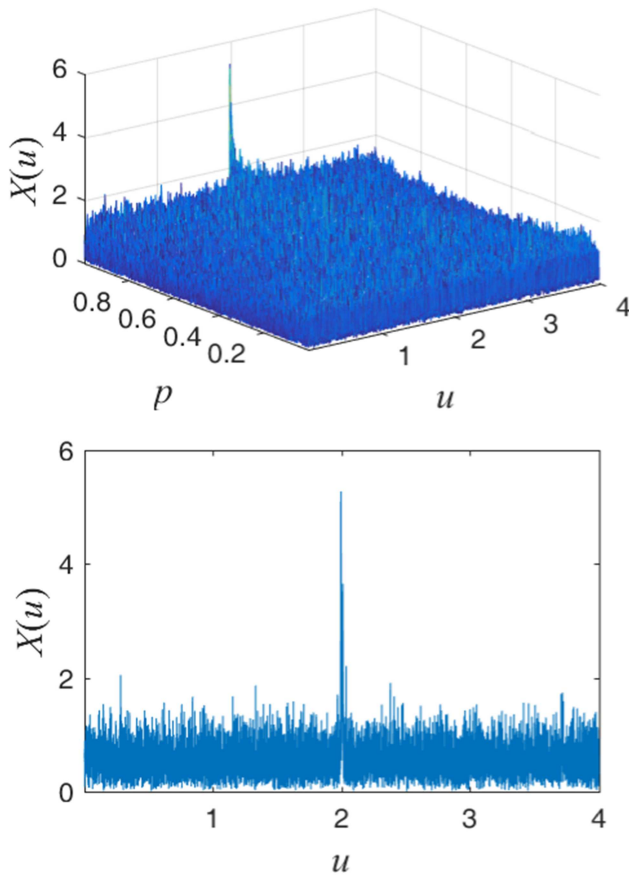


FIG. 2. The amplitude spectra of the raw signal in the fractional Fourier domain for different orders and at an optimal order. The simulation parameters are  $A = 0.3$  and  $\alpha = 1.57$ .

A. Introduction of CMGA

The CMGA is a kind of improved genetic algorithm based on the cloud model theory. The cloud model is a conversion model that can implement a transformation between qualitative concepts and quantitative values. Among the cloud models, the normal cloud model is the most commonly used that follows a normal distribution. It is defined as a universe set  $U$  that includes random numbers with a stable tendency.  $U$  is related to a qualitative concept  $C$ . The overall property of  $C$  can be described as  $C(Ex, En, He)$  by three numerical characters, that is, expected value  $Ex$ , entropy  $En$ , and hyper-entropy  $He$ . The certainty degree of  $x$  on  $C$  is represented as

$$\mu(x) = \exp\left(-\frac{(x - Ex)^2}{2En'^2}\right), \tag{12}$$

where  $x$  follows the normal distribution with mean value  $Ex$  and variance  $En'^2$ .  $En'$  also follows the normal distribution, and its mean value and variance are  $En$  and  $He^2$ , respectively. The specific digital characteristics of the cloud is shown in Fig. 6.

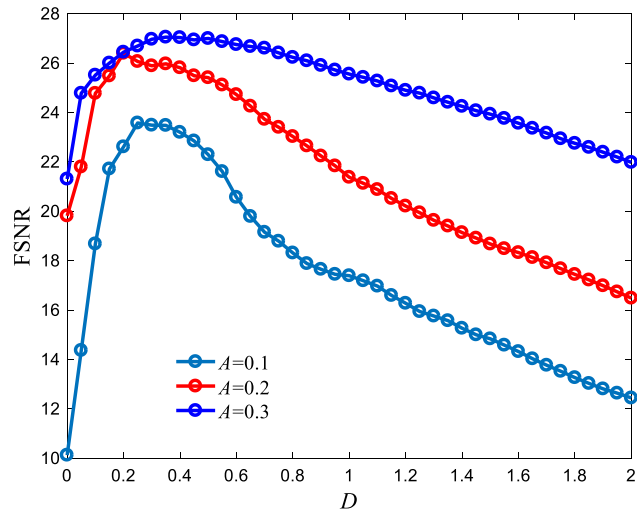


FIG. 3. Fractional signal-to-noise vs the noise intensity for three different raw signals. The simulation parameters are  $\beta = 80$ ,  $a = 1$ , and  $b = 1$ .

The normal cloud generator is the generator that produces a normal cloud model. In the algorithm, the normal cloud generator is applied in genetic crossover operation and mutation operation. Owing to the properties of randomness and stable tendency of the cloud model, the CMGA overcomes the drawbacks of the traditional genetic algorithm, and it has a good global search ability and fast convergence speed. The main procedures of the CMGA are

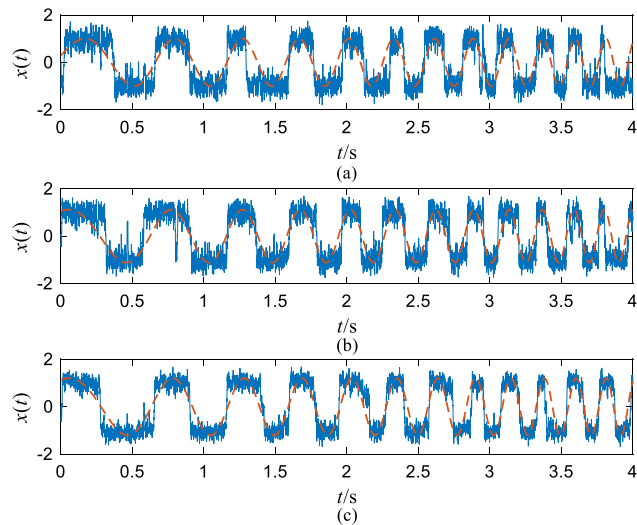
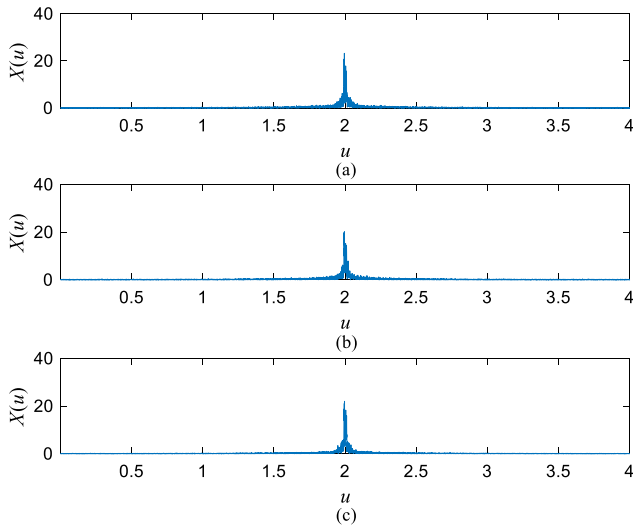


FIG. 4. The optimal system outputs after SR. The solid lines represent the outputs, and the dashed lines represent the signals after fitting. (a)  $A = 0.1$ , (b)  $A = 0.2$ , and (c)  $A = 0.3$ . The simulation parameters are  $\beta = 80$ ,  $a = 1$ , and  $b = 1$ .



**FIG. 5.** The fractional Fourier spectra for the system outputs. The simulation parameters are  $\beta = 80$ ,  $a = 1$ , and  $b = 1$ . (a)  $A = 0.1$ , (b)  $A = 0.2$ , and (c)  $A = 0.3$ .

described in detail as follows. Figure 7 illustrates the flow chart of the CMGA.

### 1. Genetic encoding

A chromosome represents an individual, which carries a potential solution to an optimization problem. Thus, for the  $d$ -variable optimization problem, each chromosome is encoded into a string in the process of genetic encoding.

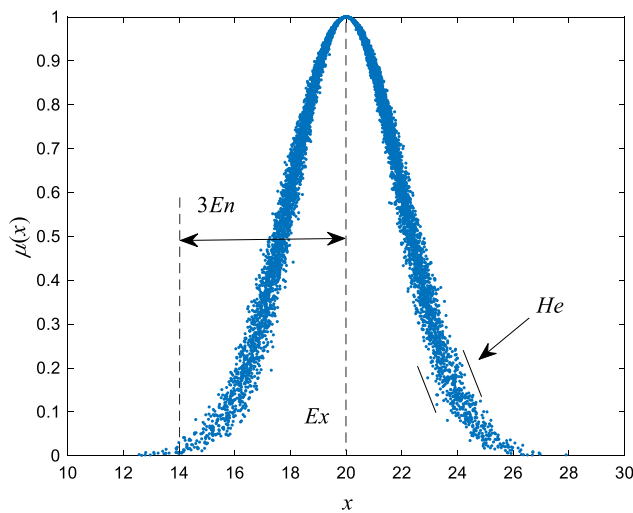


**FIG. 6.** The digital characteristics of the cloud model. The simulation parameters are  $En = 2$ ,  $Ex = 20$ , and  $He = 0.15$ .

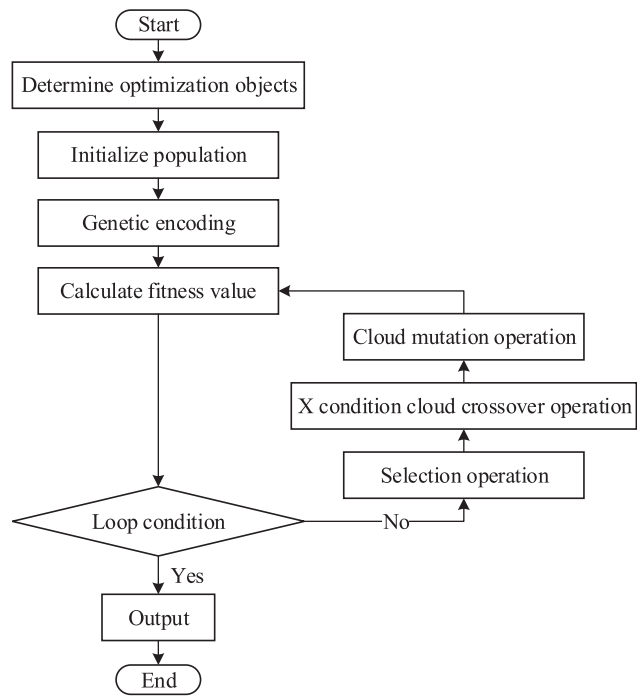


**FIG. 7.** The flow chart of the CMGA.

### 2. Selection operation

As the first step of reproduction of the population, the selection operation is a process that stochastically selects a part of individuals from the population in order to directly enter the next population. Here, the roulette wheel method, also known as fitness proportionate selection, is chosen as the individual selection method. The method being able to achieve selection is mainly based on the fitness value of an individual. The individual with a higher fitness will be more likely to be copied into the next population. Therefore, a selection operation can avoid the loss of the best individual during evolutions to some extent.

### 3. Crossover operation

A cloud crossover operator simulates a process that offspring individuals inherit parts of parents based on the theory of a cloud model. The crossover operator is realized by the X conditional cloud generator algorithm, which is described as follows.

Step 1: Calculate the average of the fitness of parent individuals, denoted as  $Ex = (f_a + f_b)/2$ .

Step 2: Generate a random number  $En'$  and let  $En$  be the mean value and  $He^2$  be the variance.  $En = m_1(F_{max} - F_{min})$  and  $He = n_1En$ , where  $m_1$  and  $n_1$  are control coefficients.  $F_{max}$  and  $F_{min}$  are the maximum and minimum of the fitness values in the parent population, respectively.

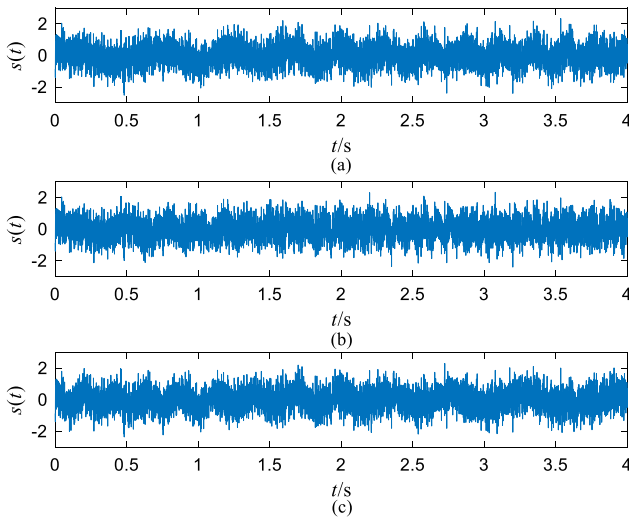


FIG. 8. Several tested raw signals with different unknown LFM signals: (a) signal 1, (b) signal 2, and (c) signal 3.

Step 3: Calculate cloud crossover operator as

$$p_{cr} = \begin{cases} t_1 e^{-\frac{(f-E_x)^2}{2En'}}, & f \geq \bar{F}, \\ t_2, & f < \bar{F}, \end{cases} \quad (13)$$

where  $\bar{F}$  is the average of the fitness of the parent population,  $f = \max(f_a, f_b)$ , and  $t_1$  and  $t_2$  are constants.

Therefore, according to the algorithm, the cloud generator will provide the crossover probability of the parents chosen randomly,  $p_{cr}$ , and a random number RAND. When  $p_{cr} > \text{RAND}$ , the crossover operation is performed by randomly choosing a site along the length of the chromosome. The two offspring individuals are produced by employing an X-condition cloud generation algorithm.

#### 4. Mutation operation

The mutation operator simulates a process of altering one or more gene values in a chromosome from its initial state, analogous to biological mutation. It ensures genetic diversity from one generation to the next so that it can make the algorithm to jump out of the local optimum. The mutation operation based on a cloud model is specifically as follows.

Step 1: Suppose the average of the fitness of a single parent individual is  $Ex$ , denoted as  $Ex = f_a$ .

Step 2: Generate a random number  $En'$  and let  $En$  be the expectation value and  $He^2$  be the variance.  $En = m_2(F_{\max} - F_{\min})$  and  $He = n_2 En$ , where  $m_2$  and  $n_2$  are control coefficients.

Step 3: Calculate the cloud mutation operator as

$$p_{mt} = \begin{cases} s_1 e^{-\frac{(f-E_x)^2}{2En'}}, & f \geq \bar{F}, \\ s_2, & f < \bar{F}, \end{cases} \quad (14)$$

where  $s_1$  and  $s_2$  are constants as well.

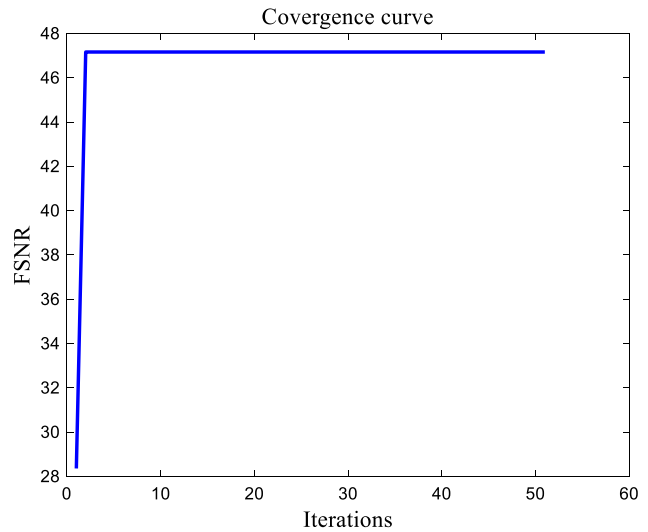


FIG. 9. The convergence curve of the CMGA.

The algorithm also performs X-condition cloud generator to generate offspring individual. Similar to crossover operation, the individual is updated by comparing  $p_{mt}$  with RAND.

#### B. Numerical optimization experiment

Based on the excellent performance of a cloud based genetic algorithm, we use it to optimize the parameters in order to achieve an adaptive SR. First, three different unknown LFM signals with some noise are given in Fig. 8.

Then, the time scale and system parameters are optimized by using the algorithm and here  $d = 3$ . Note that the loop condition here is that iteration time reaches 50. Figure 9 shows that FSNR almost reaches the optimal value (nearly 50) when iteration is  $< 10$ . This illustrates the better convergence and higher retrieval efficiency of the algorithm.

Through optimization, the system parameters that achieve an adaptive SR are obtained. Table I lists the results after optimization and the related parameters of the LFM signals in detail. According to the obtained values of parameters, SR outputs and the fitted curves are plotted in Fig. 10. Apparently, the hidden LFM signal can be recognized. In addition, the amplitude of the output is more than the one of the pure LFM signal, which means the LFM signal hidden in the raw signal is enhanced. To sum up, with the help of the

TABLE I. Optimization results and some related parameters settings.

	$a$	$b$	$D$	$\beta$	$A$	$\gamma$	$f_0$	$\phi$
Signal 1	0.8229	1.2678	0.2	75.1200	0.3	1	1	0
Signal 2	0.0694	0.8850	0.2	19.9897	0.3	4	1	0
Signal 3	0.0116	1.1089	0.2	73.3166	0.3	-1	5	0

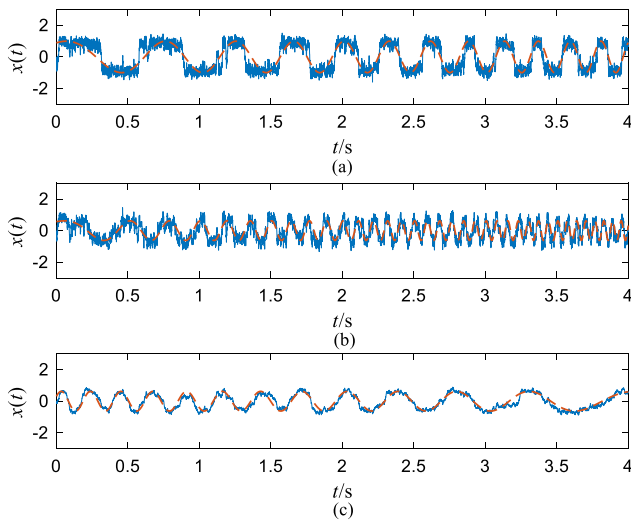


**FIG. 10.** Adaptive SR outputs through CMGA. The solid lines represent the outputs, and the dashed lines represent the signals after fitting. (a) Signal 1, (b) signal 2, and (c) signal 3.

CMGA, an adaptive SR can be easily achieved in order to recover the unknown LFM signal from the raw signal.

#### IV. CONCLUSION

This study proposes a new index, FSNR, so that the hidden LFM signal in the noise background can be characterized. In the process of calculating the index, the FRFT needs to be used so that the raw signal can be transformed into the optimal fractional domain. Then, in the optimal fractional domain, the value of the index is calculated. The numerical results indicate that the LFM signal in the raw signal can be effectively measured. In other words, it describes the energy of the hidden LFM signal well, especially when the signal in the noise is unknown.

Since the instantaneous frequency of the LFM signal varies with time, the general scale transformation is adopted so that the appropriate system parameters can be obtained. Then guided by the index, SR can occur and is able to recover the unknown LFM signal from the raw signal. By adjusting the appropriate parameters, not only the submerged LFM signal can be identified but also the signal can be enhanced because the noise energy is transferred to the signal. In addition, in order to improve the SR performance in signal processing, an adaptive SR is implemented based on the CMGA so that the better value of the time scale and the system parameters can be quickly and easily searched.

To sum up, the results of this study allow not only to achieve the detection of the unknown LFM signal but also to remove the noise interference and quickly achieve the waveform recovery of the unknown LFM signal.

#### ACKNOWLEDGMENTS

The project was supported by the National Natural Science Foundation of China (NNSFC) (Grant No. 11672325), the Priority Academic Program Development of Jiangsu Higher Education Institutions, the Top-notch Academic Programs Project of Jiangsu Higher Education Institutions, the Spanish State Research Agency (AEI), and the European Regional Development Fund (ERDF) under Project No. FIS2016-76883-P.

#### REFERENCES

- <sup>1</sup>R. Benzi, A. Sutera, and A. Vulpiani, *J. Phys. A Math. Gen.* **14**, L453 (1981).
- <sup>2</sup>P. Hänggi, *ChemPhysChem* **3**, 285 (2002).
- <sup>3</sup>A. Patel and B. Kosko, *IEEE Trans. Neural Netw.* **19**, 1993 (2008).
- <sup>4</sup>A. Dari, B. Kia, A. R. Bulsara, and W. L. Ditto, *Chaos* **21**, 047521 (2011).
- <sup>5</sup>E. Yilmaz, M. Uzuntarla, M. Ozer, and M. Perc, *Physica A* **392**, 5735 (2013).
- <sup>6</sup>Y. Hirano, Y. Segawa, T. Kawai, and T. Matsumoto, *J. Phys. Chem. C* **117**, 140 (2013).
- <sup>7</sup>J. Peng, L. Zheng, J. Li, and G. Hui, *Food Chem.* **197**, 1168 (2016).
- <sup>8</sup>F. Monifi, J. Zhang, S. K. Ozdemir, B. Peng, Y. X. Liu, F. Bo *et al.*, *Nat. Photonics* **10**, 399 (2016).
- <sup>9</sup>Y. Qin, Y. Tao, Y. He, and B. Tang, *J. Sound Vib.* **333**, 7386 (2014).
- <sup>10</sup>Y. Xu, J. Wu, L. Du, and H. Yang, *Chaos Soliton. Fract.* **92**, 91 (2016).
- <sup>11</sup>Y. Zhang, Y. Jin, and P. Xu, *Chaos* **29**, 023127 (2019).
- <sup>12</sup>D. W. Huang, J. H. Yang, J. L. Zhang, and H. G. Liu, *Proc. Inst. Mech. Eng. C* **232**, 2352 (2017).
- <sup>13</sup>X. L. Liu, H. G. Liu, J. H. Yang, G. Litak, G. Cheng, and S. Han, *Mech. Syst. Signal Process.* **96**, 58 (2017).
- <sup>14</sup>P. Xia, H. Xu, M. Lei, and Z. Ma, *Meas. Sci. Technol.* **29**, 085002 (2018).
- <sup>15</sup>Z. Qiao, Y. Lei, and N. Li, *Mech. Syst. Signal Process.* **122**, 502 (2019).
- <sup>16</sup>S. Lu, Q. He, and J. Wang, *Mech. Syst. Signal Process.* **116**, 230 (2019).
- <sup>17</sup>G. A. Patterson, A. F. Goya, P. I. Fierens *et al.*, *Physica A* **389**, 1965 (2010).
- <sup>18</sup>J. Liu, Z. Li, L. Guan, and L. Pan, *IEEE Commun. Lett.* **18**, 427 (2014).
- <sup>19</sup>J. Liu and Z. Li, *IET Image Process.* **9**, 1033 (2015).
- <sup>20</sup>D. V. Dylov and J. W. Fleischer, *Nat. Photonics* **4**, 323 (2010).
- <sup>21</sup>X. Li, G. Cao, and H. Liu, *AIP Adv.* **4**, 047111 (2014).
- <sup>22</sup>B. Le, Z. Liu, and T. Gu, *Int. J. Wavelets Multiresolut. Inf. Process.* **8**, 313 (2010).
- <sup>23</sup>J. Zheng, H. Liu, and Q. H. Liu, *IEEE Trans. Signal Process.* **65**, 6435 (2017).
- <sup>24</sup>A. Serbes, *IEEE Trans. Aerosp. Electron. Syst.* **54**, 848 (2017).
- <sup>25</sup>W. Wang, Y. Qiao, A. Yang, and P. Guo, *IEEE Photonics J.* **9**, 1 (2017).
- <sup>26</sup>D. Zhao and M. Luo, *Optik* **127**, 4405 (2016).
- <sup>27</sup>L. Lin, H. Wang, W. Lv, and S. Zhong, *Mech. Syst. Signal Process.* **76**, 771 (2016).
- <sup>28</sup>L. Lin, H. Wang, and W. Lv, *Nonlinear Dyn.* **88**, 1361 (2017).
- <sup>29</sup>L. Lin, L. Yu, H. Wang, and S. Zhong, *Commun. Nonlinear Sci. Numer. Simul.* **43**, 171 (2017).
- <sup>30</sup>C. Dai, Y. Zhu, W. Chen, and J. Lin, *Acta Electron. Sin.* **35**, 1419 (2007).
- <sup>31</sup>W. Zang, L. Ren, W. Zhang, and X. Liu, *Future Gener. Comput. Syst.* **81**, 465 (2018).